

# SYNTHESIS AND PHYSICOCHEMICAL PROPERTIES OF ESTOLIDE ESTER AND AMIDE MADE FROM USED COOKING OIL AS BIO-LUBRICANT

SENG SOI HOONG<sup>1\*</sup>; MOHD ZAN ARNIZA<sup>1</sup>; NEK MAT DIN NIK SITI MARIAM<sup>1</sup>; ABU HASSAN NOOR ARMYLISAS<sup>1</sup>; SOOK WAH TANG<sup>1</sup>; TUAN ISMAIL TUAN NOOR MAZNEE<sup>1</sup> and SHOOT KIAN YEONG<sup>1</sup>

## ABSTRACT

*Palm-based used cooking oil (UCO) is an inexpensive material that could be used as a bio-lubricant. However, its use as a bio-lubricant is limited by its inferior cold flow and oxidation stability properties. This study shows an approach to make bio-lubricant base oil from UCO that displayed good cold flow and oxidation stability. UCO was saponified and hydrolysed to yield a mixture of fatty acids, which was subsequently reacted with hydrogen peroxide and acetic acid to generate an estolide mixture with hydroxyl and carboxylic acid groups. The hydroxyl groups of the estolide mixture were end-capped with lauric acid, while its carboxylic acid groups were converted to either ester or amide functionality with 2-ethylhexanol and dibutylamine, respectively. Physicochemical properties evaluation revealed that the saturated branched structure of estolide ester and amide contributed to improved pour point (-12°C) and better oxidation stability up to 200°C as compared to UCO. Additionally, the estolide ester and amide exhibited a better viscosity index and pour point than a commercial mineral oil lubricant. The estolide ester can be classified as ISO VG 68 base oil, while the estolide amide displayed a higher viscosity grade (ISO VG 150) due to the presence of dibutylamide moiety.*

**Keywords:** esterification, kinematic viscosity, oxidation stability, palm oil, pour point.

**Received:** 30 March 2022; **Accepted:** 29 August 2022; **Published online:** 3 October 2022.

## INTRODUCTION

The global consumption of oils and fats in 2021 was estimated to be about 209 million tonnes and palm oil was the most consumed oil at about 73 million tonnes, in which 90% of palm oil was consumed as food while the remaining 10% was used for non-food purposes (Shahbandeh, 2022). One of the many ways to consume palm oil is to use it as frying oil for food preparation (Parveez *et al.*, 2021), but after a certain duration, the frying oil is unfit for that purpose and will be discarded as used cooking oil (UCO). A study estimated that 26% of globally consumed oils could end up as UCO, which could amount to 54 million tonnes based on 208 million tonnes of consumed oils in 2020 (Orjuela and Clark, 2020).

In consideration of the massive amount of UCO, proper disposal of UCO is crucial for many countries as a large portion of UCO was deliberately released into the environment, which creates many ecological problems (Ahmed and Hossain, 2020). Therefore, it is important to find uses for UCO to resolve problems associated with the disposal of UCO. Additionally, the use of UCO to make other products also conform to the principles of circular economy, which is gaining wider acceptance than the conventional linear economy (Orjuela and Clark, 2020).

Many scientists have evaluated UCO as feedstock to produce various products such as biodiesel (Milano *et al.*, 2022), surfactants and bio-lubricant (Orjuela and Clark, 2020). Among these potential applications, bio-lubricant is a value-added product that represents the circular economy and the idea of generating wealth from waste. Furthermore, the relatively inexpensive UCO could help to mitigate the issue of high material costs associated with bio-lubricant, which is a

<sup>1</sup> Malaysian Palm Oil Board,  
6 Persiaran Institusi, Bandar Baru Bangi,  
43000 Kajang, Selangor, Malaysia.

\* Corresponding author e-mail: [sengsoi@mpob.gov.my](mailto:sengsoi@mpob.gov.my)

major barrier to market acceptance of bio-lubricant (Zhang *et al.*, 2020).

The properties of a bio-lubricant made from UCO are very dependent on the fatty acid composition of UCO and the chemical process employed to modify the UCO. Specifically, UCO with high content of saturated fatty acids such as palmitic acid will generate bio-lubricant with undesirable cold flow properties but satisfactory oxidation stability (Heikal *et al.*, 2017). Conversely, bio-lubricant made with UCO that is rich in unsaturated fatty acids will exhibit good cold flow properties but inferior oxidation stability due to the presence of the alkene group (Li and Wang, 2015).

Hence, chemical modification conducted on UCO is designed to overcome drawbacks related to its chemical structure. One of the most common methods employed to modify UCO is transesterification with trimethylolpropane, which converts UCO to polyol esters that enhance the cold flow properties of resultant polyol esters. For example, Wang *et al.* (2014) reported a process that converted a UCO rich in oleic acid to trimethylolpropane esters, which displayed similar cold flow properties in comparison with ISO VG32 mineral oil-based lubricant. Nevertheless, the prepared polyol esters have alkene groups that are susceptible to oxidation degradation, which will reduce the service life of the resultant lubricants. Hence, it will be advantageous to prepare bio-lubricant from UCO that has a minimal alkene group.

A prominent method to convert vegetable oils into bio-lubricants with minimal alkene group is through the formation of estolide (Isbell, 2011; Salimon *et al.*, 2012). Generally, estolide is prepared from unsaturated fatty acids such as oleic acid through a reaction with strong acids. Cermak *et al.* (2015) reported that a mixture of saturated fatty acids and oleic acid was converted to estolide in the presence of perchloric acid. Subsequently, the prepared estolide was reacted with a branched alcohol that yielded estolide ester, which showed excellent cold flow properties and acceptable oxidation stability. Nonetheless, the use of perchloric acid poses safety hazards to the community because it is known to form an explosive mixture in addition to its corrosive nature and should be substituted with a less hazardous material whenever possible (Schilt, 1979).

Alternatively, we have recently reported a synthetic method to make polyhydroxy estolide (PE) from oleic acid through a reaction with hydrogen peroxide and acetic acid, which is relatively safer in comparison with the perchloric acid method (Hoong *et al.*, 2021). Then, the prepared PE was further converted to yield estolide ester and amide, which exhibited properties comparable to commercial samples in terms of pour point, oxidation stability,

viscosity index and anti-wear (Hoong *et al.*, 2020). Additionally, the estolide ester and amide were found to be readily biodegradable, which indicated that the prepared estolide ester and amide have good potential to be used as environment-friendly lubricant base oils (Hoong *et al.*, 2020). These positive results encourage further evaluation of this method on cheaper feedstocks such as palm-based UCO.

To the best of the author's knowledge, palm-based UCO has not been evaluated as feedstock for making estolide ester, albeit it is abundantly available. This could be due to the high content of saturated fatty acids in palm-based UCO that would contribute to inferior cold flow properties of the resultant lubricant, and hence discourage the evaluation of palm-based UCO as feedstock. Nonetheless, it will be advantageous to produce a bio-lubricant from palm-based UCO that exhibits properties comparable to commercial lubricants. Therefore, this article reports the synthesis of PE from palm-based UCO through reaction with hydrogen peroxide and acetic acid. Subsequently, the prepared PE was converted to estolide ester and amide which exhibited properties comparable to commercial lubricant. The results of this article will help to establish a safe and feasible method to produce bio-lubricant from palm-based UCO.

## MATERIALS AND METHODS

### Materials

Used cooking oil was obtained from a local restaurant located in Kajang, Selangor, Malaysia. Fresh cooking oil (Alif brand, Sime Darby Oils Trading Sdn. Bhd.) was purchased from a local grocery store. Sodium hydroxide (98%), phosphoric acid (85%), hydrogen peroxide (50% in H<sub>2</sub>O), acetic acid glacial (99%), lauric acid (98%), dibutylamine (99%) and 2-ethylhexanol (99%) were purchased from Sigma Aldrich (St Louis, MO, USA). All acquired chemicals were used without further purification unless otherwise stated.

### Characterisation Methods

All measurements were performed in triplicate and data were reported as the mean  $\pm$  standard deviation. Gas chromatography (GC) analysis was conducted using Agilent 7890B GC System equipped with Agilent J&W HP-88 (60 m x 0.25 mm x 0.2  $\mu$ m) capillary column and flame ionisation detector. Fatty acid methyl esters were prepared from UCO according to AOCS's official method Ce 2-66 (AOCS, 2009). Temperature programme used for the GC analysis: oven temperature, 150°C; initial temperature, 150°C; heating rate at 3°C min<sup>-1</sup>; final temperature, 210°C; injector temperature, 250°C and

detector temperature, 250°C. Helium was supplied at a rate of 0.8 mL min<sup>-1</sup>. Fatty acid methyl esters solution (1 µL) was injected into the GC system.

FTIR spectra were recorded on a Perkin-Elmer Spectrum100 FTIR spectrometer. Samples were analysed as a thin film over a diamond attenuated total reflectance (ATR) top plate. Spectra were recorded in a range of 650-4000 cm<sup>-1</sup> and the average value of eight scans at 4 cm<sup>-1</sup> resolution was recorded for each sample.

Proton (<sup>1</sup>H) and carbon (<sup>13</sup>C) nuclear magnetic resonance (NMR) spectra were acquired on JOEL JNM-ECZ600R at 600 MHz and 150 MHz, respectively at 25°C. Samples were dissolved in deuterated NMR solvents with approximately 10% w/v solution. Chemical shifts were referenced to internal standard tetramethylsilane (TMS).

Gel permeation chromatography (GPC) was performed with a Polymer Laboratories PL-GPC 50 Plus equipped with a combined detector of differential refractive index (DRI)/viscometer. The sample (2 mg mL<sup>-1</sup>) was dissolved in tetrahydrofuran (THF) and was analysed using a set of Phenogel columns that measure molecular weight in the range of 10<sup>2</sup>-10<sup>6</sup> Da. The sample was eluted in THF at a flow rate of 1 mL min<sup>-1</sup>. The GPC was calibrated using polystyrene standards with a range from 162 to 1 × 10<sup>5</sup> Da.

Wet chemical analysis was performed in accordance with the AOCS official methods (AOCS, 2009): Acid value (AV), Cd 1a-64; hydroxyl value (OHV), Cd 13-60; iodine value (IV), Cd 1d-92; saponification value (Sap V), Cd 3-25; oxirane oxygen content (OOC), Cd 9-57.

Kinematic viscosity measurements were carried out in accordance with ASTM D445 standard method at 40°C and 100°C using calibrated Ubbelohde viscometer tubes and a Normalab NVB Classic viscosity bath with a constant temperature. The viscosity index was calculated in accordance with the standard method ASTM D2270-93.

Pour point and cloud point measurements were conducted in accordance with standard methods ASTM D97 and ASTM D2500, respectively. Measurements were carried out using a Normalab CPP Classic test cabinet with integrated cooling.

The oxidation onset temperature (OOT) analysis was conducted in accordance with the standard method ASTM E2009 using a DSC Q20P thermal analyser equipped with a Tzero pressure DSC cell acquired from TA Instruments.

The anti-wear properties of samples were evaluated in accordance with the ASTM 4172 (Four-ball method). The test was carried out using a four-ball tester TR-30L made by DUCOM Instrument, India. The test balls with product code RB-12.7/G20W were acquired from SKF Malaysia Sdn. Bhd.

### Saponification of Used Cooking Oil (UCO) and Hydrolysis of Soap

Suspended particles in UCO were removed by filtration through a normal sieve. The filtered UCO (1200 g) was poured into a 10 L reactor equipped with a motor stirrer. The UCO was heated to 80°C and sodium hydroxide solution (3 M, 2000 mL) was added to the UCO. The mixture was stirred vigorously (300 rpm) and heated at 80°C. After 4 hr of reaction, phosphoric acid solution (4 M, 2000 mL) was added, and the reaction was continued for another 2 hr. Next, the reaction mixture was left to separate into two layers. The aqueous layer was discarded, and the organic layer was washed twice with deionised water (1500 mL). Thereafter, the organic layer was dried over anhydrous MgSO<sub>4</sub> to yield a mixture of fatty acids (1021 g, 95% yield).

### Synthesis of Estolide Mixture from UCO-based Fatty Acids Mixture

The fatty acids mixture prepared from UCO (500 g) and acetic acid glacial (66 g) were charged into a 2 L reactor equipped with a motor stirrer. The reaction mixture was heated to 80°C and then hydrogen peroxide (190 mL) was added dropwise. The reaction mixture was stirred vigorously (300 rpm) and heated at 80°C for 8 hr. Thereafter, the reaction mixture was left to separate into two layers and the aqueous layer was discarded. The organic layer was washed twice with deionised water (250 mL). The organic layer was then dried over anhydrous MgSO<sub>4</sub> to yield a solid labelled as estolide mixture (491 g, 95% yield).

### Synthesis of Lauric Acid-capped Estolide (LaE)

Estolide mixture (450 g, 0.955 mole of OH, OHV = 119 mg KOH g<sup>-1</sup>) and lauric acid (68 g, 0.34 mole) were charged into a reaction flask equipped with a magnetic stirrer and distillation apparatus. The reaction mixture was stirred and heated at 200°C for 8 hr. Subsequently, the product was diluted with ethyl acetate (400 mL) after it was cooled to room temperature and was dried over anhydrous MgSO<sub>4</sub>. The solvent was removed to yield a viscous yellowish liquid labelled as lauric acid-capped estolide (485 g, 97% yield).

### Synthesis of 2-ethylhexyl Ester of Lauric Acid-capped Estolide (2EHLaE)

Lauric acid-capped estolide (200 g, 0.32 mole of CO<sub>2</sub>H, AV = 89 mg KOH g<sup>-1</sup>) and 2-ethylhexanol (2EH) (90 g, 0.69 mole) were charged into a reaction flask equipped with a magnetic stirrer and Dean-Stark apparatus. The mixture was stirred and heated to 200°C for 10 hr. Thereafter, excess

2-ethylhexanol was removed from the product by vacuum distillation. Then, the product was diluted with ethyl acetate (200 mL) and dried over anhydrous  $MgSO_4$ . The solvent was removed to yield a viscous yellowish liquid labelled as 2-ethylhexyl ester of lauric acid-capped estolide (229 g, 97% yield).

### Synthesis of Dibutylamide of Lauric Acid-capped Estolide (DBALaE)

Lauric acid-capped estolide (200 g, 0.32 mole of  $CO_2H$ ,  $AV = 89 \text{ mg KOH g}^{-1}$ ) and dibutylamine (DBA) (83 g, 0.64 mole) were charged into a reaction flask equipped with a magnetic stirrer and Dean-Stark apparatus. The mixture was stirred and heated to  $200^\circ C$  for 16 hr. Subsequently, excess dibutylamine was removed from the product by vacuum distillation. Thereafter, the product was diluted with ethyl acetate (200 mL) and dried over anhydrous  $MgSO_4$ . The solvent was removed to yield a viscous yellowish liquid labelled as dibutylamide of lauric acid-capped estolide (225 g, 95% yield).

## RESULTS AND DISCUSSION

### Characterisation of Used Cooking Oil

The palm-based UCO was analysed using gas chromatography to determine its fatty acid composition (FAC) and it was also subjected to wet chemistry analyses to ascertain a few

properties. The properties of UCO are listed in *Table 1* together with local fresh cooking oil for comparison purposes. Fresh cooking oil is a refined, bleached and deodorised palm olein (RBDPOo), which is a typical cooking oil used in Malaysia for food preparation that would eventually end up as UCO.

Referring to *Table 1*, the acid value (AV) of UCO ( $5.82 \text{ mg KOH g}^{-1}$ ) was significantly higher than AV of fresh cooking oil ( $0.17 \text{ mg KOH g}^{-1}$ ) due to the hydrolysis of palm olein's triglycerides molecules that occurred during the food frying process, which generated free fatty acids that contributed to the observed high AV of UCO (Lam *et al.*, 2010). The AV of UCO would vary depending on the duration the cooking oil is used as a medium for the food frying process and the type of food preparation. A typical range of AV of palm olein-based UCO would be between 2 to  $21 \text{ mg KOH g}^{-1}$  as reported in the literature (Cheah *et al.*, 2016; Loh *et al.*, 2006).

The iodine value (IV) analysis quantifies the amount of alkene group in vegetable oil, in which a higher IV denotes a higher amount of alkene group in the vegetable oil. Results from *Table 1* show that the IV of UCO was slightly lower than fresh cooking oil due to oxidation of the alkene group by molecular oxygen during the food frying process (Kulkarni and Dalai, 2006). Nevertheless, the IV of UCO was found acceptable as feedstock for making estolide because it had an adequate amount of alkene group that can be modified to generate estolide.

TABLE 1. PROPERTIES OF FRESH COOKING OIL AND USED COOKING OIL

Analysis	Unit	Fresh cooking oil	Used cooking oil
Acid value	mg KOH $g^{-1}$	$0.17 \pm 0.05$	$5.82 \pm 0.05$
Iodine value	$g I_2 100 g^{-1}$	$58.90 \pm 0.40$	$54.60 \pm 0.30$
Moisture content	wt%	$0.05 \pm 0.01$	$0.30 \pm 0.03$
Saponification value	mg KOH $g^{-1}$	$195.20 \pm 0.90$	$203.00 \pm 1.20$
<b>Fatty Acid Composition</b>			
Lauric acid, C12:0	wt%	$0.20 \pm 0.01$	$0.20 \pm 0.01$
Myristic acid, C14:0	wt%	$0.90 \pm 0.02$	$1.00 \pm 0.03$
Palmitic acid, C16:0	wt%	$36.30 \pm 0.40$	$37.30 \pm 0.40$
Palmitoleic acid, C16:1	wt%	$0.20 \pm 0.01$	$0.20 \pm 0.01$
Margaric acid, C17:0	wt%	ND*	$0.4 \pm 0.05$
Stearic acid, C18:0	wt%	$5.70 \pm 0.20$	$6.20 \pm 0.30$
Oleic acid, C18:1	wt%	$44.80 \pm 0.50$	$43.90 \pm 0.60$
Linoleic acid, C18:2	wt%	$11.10 \pm 0.30$	$10.20 \pm 0.30$
Linolenic acid, C18:3	wt%	$0.20 \pm 0.02$	$0.10 \pm 0.01$
Arachidic acid, C20:0	wt%	$0.30 \pm 0.01$	$0.30 \pm 0.02$
Eicosenoic acid, C20:1	wt%	$0.20 \pm 0.02$	$0.10 \pm 0.01$
Behenic acid, C22:0	wt%	$0.10 \pm 0.01$	$0.10 \pm 0.02$

Note: \*ND - not detected.

The FAC analysis revealed that the food frying process had increased the amount of saturated fatty acid in UCO at the expense of unsaturated fatty acids such as oleic acid due to oxidation reaction on alkene groups of cooking oil that resulted in conversion to a saturated moiety. Additionally, the FAC analysis also detected a small amount of margaric acid in UCO, which did not originate from RBDPOo but most likely originated from animal fat introduced into UCO during the food frying process. Nonetheless, the small amount of margaric acid has an insignificant impact on the performance of the targeted bio-lubricant. Overall, the results of analyses conducted on UCO suggested that the palm-based UCO is suitable to be used as feedstock to produce estolide.

### Preparation of UCO-based Fatty Acids Mixture

The UCO was saponified with excess sodium hydroxide solution to yield soap and glycerol. Subsequently, the soap was hydrolysed with phosphoric acid to generate a mixture of fatty acids. Results of the analyses showed that the mixture of fatty acids had an IV ( $54 \text{ g I}_2 100 \text{ g}^{-1}$ ) like UCO and an AV of  $202 \text{ mg KOH g}^{-1}$ . Additionally, the mixture of fatty acids had a similar FAC in comparison with UCO, which indicated that the saponification of UCO and hydrolysis of soap did not change the FAC of UCO as expected.

The subsequent synthesis of estolide from the UCO-based fatty acids mixture is dependent on the alkene groups of the fatty acids mixture as chemical modification will occur on the alkene group and eventually affects the physicochemical properties of the resultant bio-lubricant. The FAC analysis revealed that the fatty acids mixture had about 54% of unsaturated fatty acids, in which oleic and linoleic acid were the major components. The level of unsaturated fatty acids found in the fatty acid mixture is considered sufficient to provide an adequate amount of alkene group for making estolide.

### Synthesis of Estolide Mixture from UCO-based Fatty Acids Mixture

The prepared UCO-based fatty acids mixture was reacted with a relatively safe oxidant namely hydrogen peroxide ( $\text{H}_2\text{O}_2$ ) and acetic acid to yield an estolide mixture, as shown in *Figure 1*. During the reaction,  $\text{H}_2\text{O}_2$  reacted with acetic acid, which converted it into a peroxy acid. The generated peroxy acid eventually reacted with alkene groups of fatty acids mixture and transformed the alkene group into an epoxide group. Subsequently, the epoxide groups of epoxidised fatty acids mixture were ring-opened by nucleophiles presence in the reaction mixture, namely the carboxylic acid group of fatty acids and acetic acid along with water molecule.

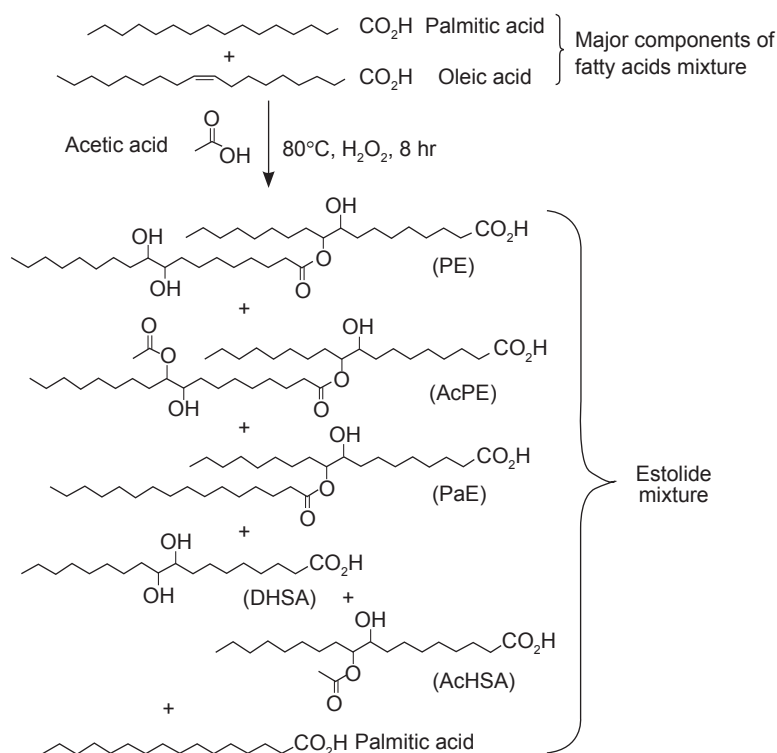


Figure 1. Synthesis of estolide mixture from UCO-based fatty acids mixture.

As a result, the epoxidation and epoxide ring-opening reactions performed on fatty acids mixture yielded a blend of compounds collectively known as estolide mixture, which comprised polyhydroxy estolide (PE), acetylated polyhydroxy estolide (AcPE), palmitic acid-capped estolide (PaE), 9,10-dihydroxystearic acid (DHSA), acetylated hydroxystearic acid (AcHSA) and unreacted saturated fatty acids such as palmitic acid.

Palmitic acid is one of the nucleophiles that can ring-open the epoxide group, which produced the compound PaE. Likewise, AcHSA and DHSA were generated from epoxide ring-opening by acetic acid and water, respectively. Meanwhile, the same epoxide ring-opening reaction with oleic acid yielded estolide with alkene group that can be further epoxidised and subsequently ring-opened with either acetic acid or water to yield AcPE and PE, respectively.

The progress of the reaction was monitored through oxirane oxygen content (OOC) analysis as shown in *Figure 2*. The OOC values increased in the first 3 hr of the reaction to a maximum of 0.81% and then gradually reduced to below 0.20% as the reaction progressed further. The OOC data suggested that epoxidation and epoxide ring-opening reactions occurred concurrently, in which the newly formed epoxide group was rapidly ring-opened by nucleophiles and this prohibited the OOC value from reaching the maximum theoretical value of 3.37%.

The conversion of the alkene group can be measured by using IV analysis, which revealed a conversion of 96% was achieved as the IV of fatty

acid mixtures was reduced from an initial value of  $54 \text{ g I}_2 100 \text{ g}^{-1}$  to less than  $2 \text{ g I}_2 100 \text{ g}^{-1}$ . Additionally, the AV of the fatty acids mixture was reduced from  $202 \text{ mg KOH g}^{-1}$  to  $152 \text{ mg KOH g}^{-1}$ , which suggested that carboxylic acid groups of the fatty acids mixture were involved in the epoxide ring-opening reaction that resulted in the formation of estolide with hydroxyl functionality.

This idea is supported by  $^1\text{H}$  NMR analysis of the estolide mixture as shown in *Figure 3a*, which exhibited a peak at 4.80 ppm that correlated with the methine proton linked to an ester group. Further analysis with  $^1\text{H}$ - $^1\text{H}$  COSY NMR showed that the methine proton peak at 4.80 ppm correlated with another methine proton of a hydroxyl group detected at 3.56 ppm, which indicated that the hydroxyl group was adjacent to the ester group due to epoxide ring-opening by a carboxylic acid group of fatty acid that formed the ester linkage of estolide's molecular structure. The GPC analysis (*Figure 4a*) revealed that the estolide mixture contained about 60% of estolides, which included PE, AcPE and PaE, with an average molecular weight of 950 Da. The other 40% of the estolide mixture comprised monomeric compounds AcHSA, DHSA and unreacted fatty acids, with an average molecular weight of 370 Da. Overall, the average molecular weight of the estolide mixture was about 740 Da.

### Synthesis of LaE

Salimon *et al.* (2011) disclosed that lubricant base oils without a hydroxyl group achieved higher oxidation stability than those with a hydroxyl group.

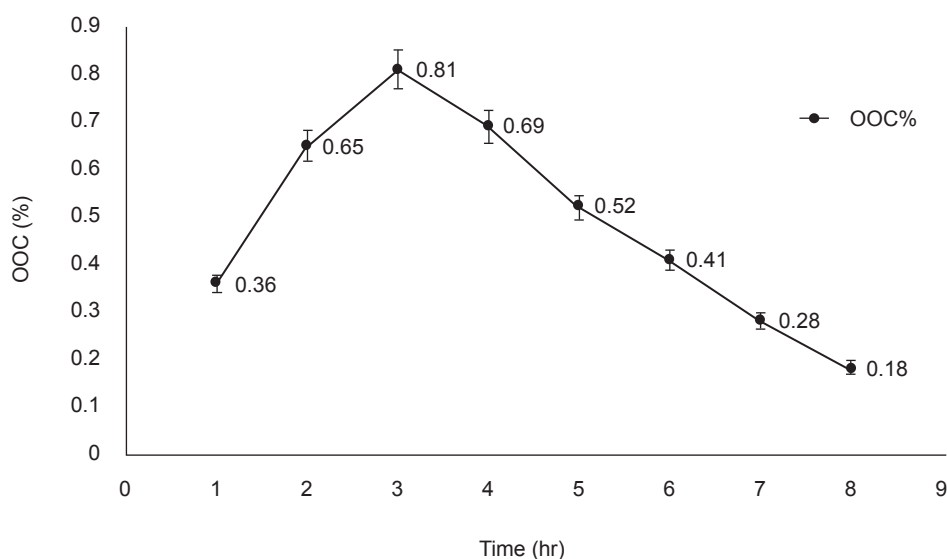


*Figure 2.* Oxirane oxygen content (OOC) of reaction mixture against time.

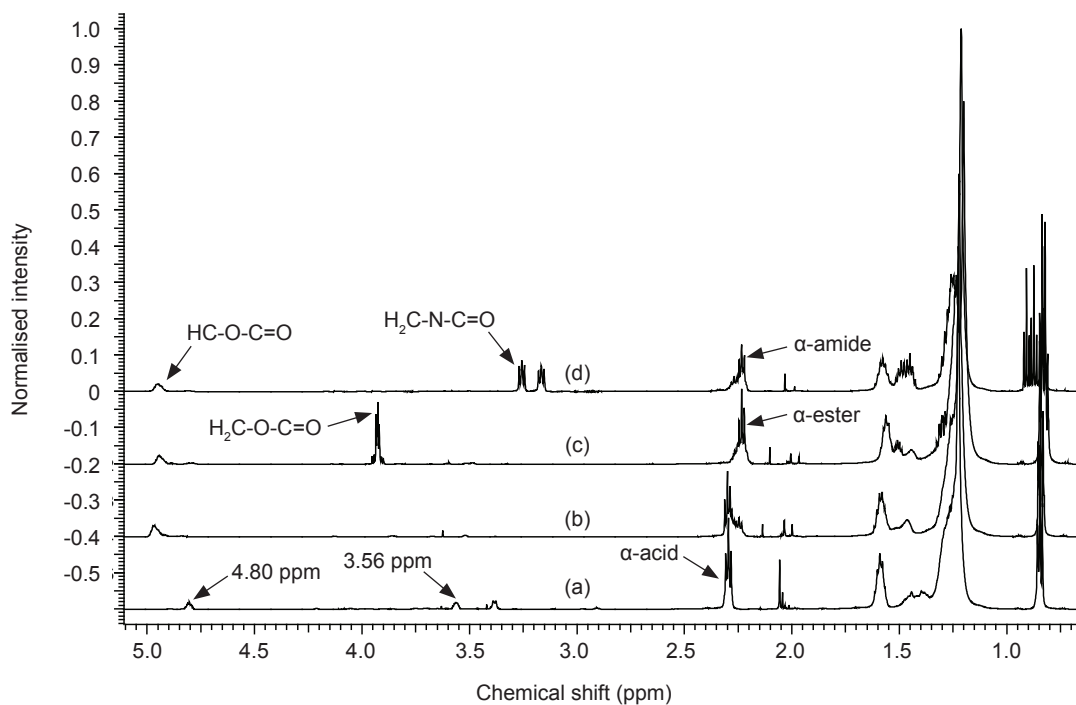


Figure 3.  $^1\text{H}$  NMR spectrum of (a) estolide mixture, (b) lauric acid-capped estolide (LaE), (c) estolide ester (2EHLaE) and (d) estolide amide (DBALaE).

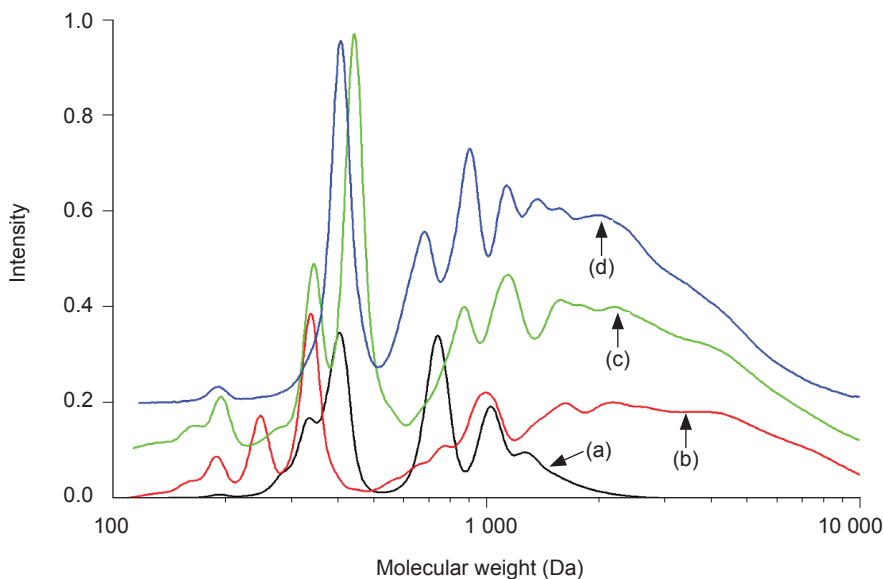


Figure 4. GPC chromatogram of (a) estolide mixture, (b) lauric acid-capped estolide (LaE), (c) estolide ester (2EHLaE) and (d) estolide amide (DBALaE).

Hence, the estolide mixture was self-esterified in combination with lauric acid (Figure 5) to transform hydroxyl groups of the estolide mixture into ester groups to attain better oxidation stability. The selection of lauric acid to end-cap the hydroxyl group was based on a study reported by Isbell (2011), which revealed that lubricant base oils made with lauric acid exhibited good cold flow properties and oxidation stability.

The amount of lauric acid used in the reaction varied from 15% to 30% (w/w) based on the amount of estolide mixture. Hydroxyl value (OHV) analysis was performed on the product and revealed that the reaction conducted with 15% of lauric acid was sufficient to convert all hydroxyl groups to ester functionality as indicated by OHV of the LaE, which was below  $5 \text{ mg KOH g}^{-1}$ . When the same reaction was conducted with

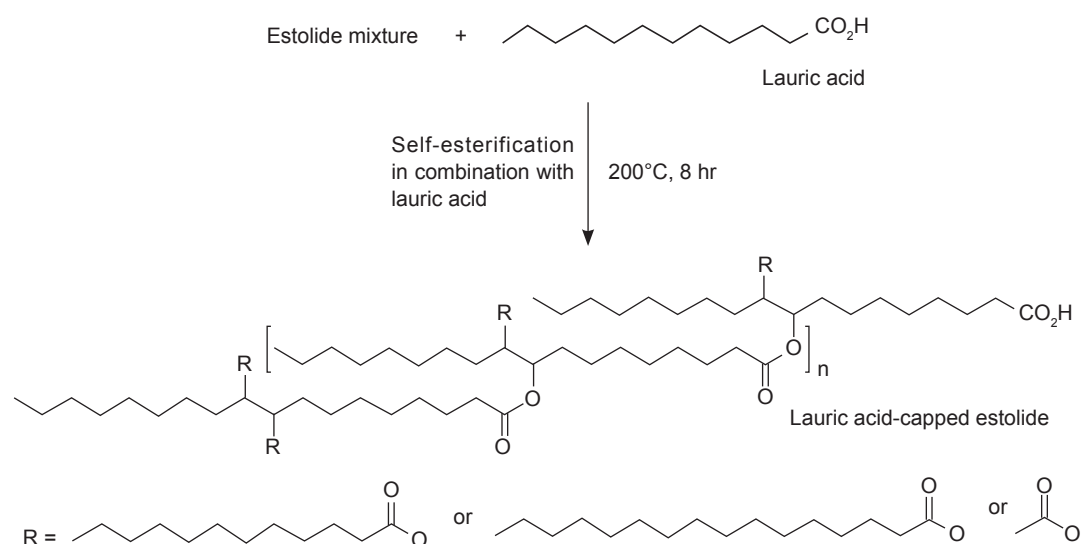


Figure 5. Synthesis of lauric acid-capped estolide (LaE).

30% lauric acid, the product displayed a layer of solid sedimentation upon storage, which suggested that 30% lauric acid was excessive for the reaction.

The conversion of the hydroxyl group of estolide mixture to the ester group was confirmed by  $^1\text{H}$  NMR analysis. Referring to Figure 3a, the two peaks that represented hydroxyl groups of estolide mixture at 3.56 ppm and 3.33 ppm were not observed in the  $^1\text{H}$  NMR spectrum of LaE (Figure 3b), which indicated that all hydroxyl groups of estolide mixture were converted to ester functionality. Moreover, a new peak was observed at 4.95 ppm in the  $^1\text{H}$  NMR spectrum of LaE (Figure 3b), which correlated with a methine proton attached to the newly formed ester group. Additionally, the methylene proton peak of  $\alpha$ -ester was observed at 2.25 ppm and all these  $^1\text{H}$  NMR data proved the formation of LaE.

Moreover, the self-esterification of the estolide mixture in combination with lauric acid not only managed to end-cap all the hydroxy groups of the estolide mixture but also increased the molecular weight of LaE through the formation of ester linkages between fatty acid molecules. The GPC analysis showed that the average molecular weight of LaE (Figure 4b) was about 1900 Da, which was more than twice the average molecular weight of the estolide mixture (Figure 4a) and the oligomeric content of LaE was about 80%, which consisted of dimer, trimer and higher oligomers of LaE, while the remaining 20% comprised unreacted monomeric fatty acids. Additionally, the GPC chromatogram of LaE (Figure 4b) also revealed that the oligomers of LaE exhibited a broad molecular weight

distribution in the range of 500 Da to 10 000 Da due to the self-esterification of the estolide mixture. It is noteworthy to mention that the presence of lauric acid and other saturated fatty acids in the reaction mixture prohibited the formation of cross-linked (gel) product, which would have formed in the self-esterification of estolide mixture without lauric acid and other saturated fatty acids as end-capping fatty acid to limit the degree of polymerisation.

### Synthesis of 2EHLaE and DBALaE

Literature (Beran, 2010) reported that ester-based bio-lubricants typically have AV lower than  $1 \text{ mg KOH g}^{-1}$  to achieve good hydrolytic stability. Therefore, carboxylic acid groups of prepared LaE were converted to ester groups through reaction with 2-ethylhexanol (2EH) as it was reported by Sammaiah *et al.* (2016) to impart good cold flow and oxidation stability. Hence, the prepared LaE was reacted with an excess amount of 2EH as shown in Figure 6 to generate a 2EHLaE. The reaction was considered completed when the AV of the product was below  $1 \text{ mg KOH g}^{-1}$ .

Alternatively, the carboxylic acid groups of LaE can be converted to amide bond, which is known to have better hydrolysis resistance in comparison with the ester group (Lee *et al.*, 2002). Thus, LaE was reacted with excess dibutylamine (DBA) to yield estolide amide with AV below  $1 \text{ mg KOH g}^{-1}$  labelled as DBALaE (Figure 6). Dibutylamine was chosen because it is a biodegradable and relatively low-cost secondary amine (Kalla *et al.*, 2014), which will form a tertiary amide with a branched structure that would impart good cold flow properties.



The  $^1\text{H}$  NMR spectrum of 2EHLaE (Figure 3c) showed a peak at 2.25 ppm that correlated with methylene protons adjacent to an ester group ( $\alpha$ -ester), while methylene protons adjacent to a carboxylic acid group ( $\alpha$ -acid) were not detected at 2.3 ppm, which indicated that all the carboxylic acid groups of LaE were completely transformed to ester functionality. Additionally, the spectrum also exhibited another peak at 3.93 ppm, which represented the methylene protons of 2EH moiety adjacent to the ester group, which proved the conversion of the carboxylic acid group to the ester group by 2EH.

As for estolide amide DBALaE,  $^1\text{H}$  NMR analysis (Figure 3d) showed two peaks at 3.26 and 3.17 ppm, which corresponded with the methylene group of dibutylamine moiety adjacent to the amide bond. The  $^1\text{H}$  NMR spectrum of DBALaE also showed that methylene protons adjacent to the amide group ( $\alpha$ -amide) were detected at 2.23 ppm, while the methylene protons adjacent to the carboxylic acid ( $\alpha$ -acid) were not detected. These results strongly suggested that all the carboxylic acid groups of LaE were converted to amide groups.

Furthermore, the GPC analysis revealed that the average molecular weight of 2EHLaE and DBALaE was slightly increased to 2000 Da (Figure 4c and 4d) in comparison with LaE due to the addition of 2EH and DBA moiety, respectively. The GPC analysis also showed that 2EHLaE and DBALaE exhibited similar chromatogram patterns in comparison with LaE. In addition, the oligomeric composition of 2EHLaE and DBALaE was about

80%, which was similar to LaE. This indicated that the esterification and amidation reactions did not alter the oligomeric composition of the reactant and eventually produced oligomers of 2EHLaE and DBALaE with molecular weights between 600 Da to 10 000 Da. On the other hand, the remaining 20% of 2EHLaE and DBALaE mainly consisted of monomeric 2-ethylhexyl ester and dibutyl amide of fatty acids, respectively.

### Evaluation of 2EHLaE and DBALaE as Lubricant Base Oil

The prepared 2EHLaE and DBALaE were subjected to a typical evaluation of lubricant properties as shown in Table 2. The properties of estolide ester and amide were compared with palm-based trimethylolpropane triesters (TMPTE) synthesised from palm oil and trimethylolpropane (Nurazira *et al.*, 2019) as well as a commercial mineral oil-based lubricant (HLP68), which serve as a benchmark for commercially acceptable properties of a lubricant. Additionally, a triglycerides-based estolide that was prepared from palm olein (Derawi and Salimon, 2013) is also included in Table 2 for comparison of lubricant properties with 2EHLaE and DBALaE. The triglyceride-based estolide (labelled as DOPO) was prepared from palm olein through several reaction steps namely epoxidation, epoxide ring-opening with water and finally esterification with oleic acid.

One of the important attributes of a lubricant is its viscosity, which directly affects its lubrication performance at operational temperature. Hence,

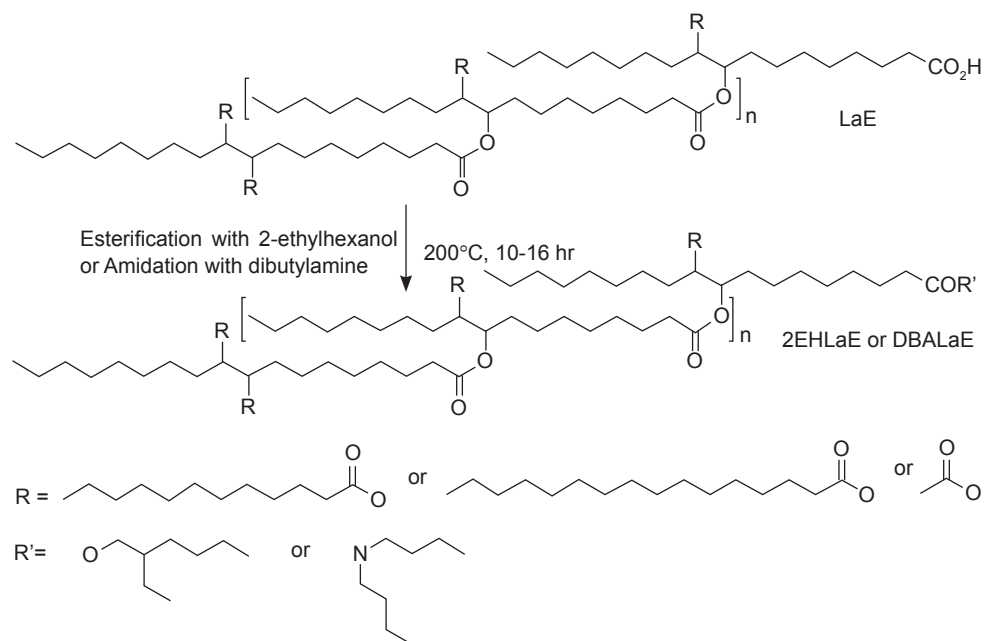


Figure 6. Synthesis of lauric acid-capped estolide ester (2EHLaE) and estolide amide (DBALaE).

TABLE 2. PHYSICOCHEMICAL PROPERTIES OF 2EHLAE, DBALAE, TMPTE, DOPO AND HLP68

Sample	KV		VI	PP (°C)	OOT (°C)	WSD (mm)
	40°C, cSt	100°C, cSt				
2EHLaE	63.1 ± 0.1	11.8 ± 0.1	190	-12.0 ± 0.0	199.8 ± 0.2	0.58 ± 0.06
DBALaE	136.2 ± 0.2	20.3 ± 0.1	169	-12.0 ± 0.0	200.3 ± 0.2	0.56 ± 0.05
TMPTE <sup>a</sup>	61.8	14.0	236	9.0	183.0	ND
DOPO <sup>b</sup>	417.5	45.4	166	-5.0	155.8	ND
HLP68 <sup>c</sup>	68.2 ± 0.2	8.8 ± 0.1	107	-6.0 ± 0.0	199.2 ± 0.1	0.60 ± 0.05

Note: KV - kinematic viscosity; VI - viscosity index; PP - pour point; OOT - oxidation onset temperature; WSD - four-ball wear scar diameter, ND - not determined.

Source: <sup>a</sup>Nurazira *et al.* (2019).

<sup>b</sup>Derawi and Salimon (2013).

<sup>c</sup>Commercial mineral oil-based lubricant.

the kinematic viscosity of a lubricant is typically measured at 40°C and 100°C to ascertain the viscosity profile of a lubricant. Consequently, lubricants are classified according to their kinematic viscosity measured at 40°C, which is known as ISO viscosity grade (ISO VG) classification. Referring to *Table 2*, the kinematic viscosities of 2EHLaE, TMPTE and HLP68 can be classified as ISO VG 68 lubricant, which is suitable to be used as a base oil for hydraulic fluid, gear oil and compressor oil.

In contrast, DBALaE exhibited significant higher kinematic viscosity at 40°C (136 cSt) than its ester counterpart and is classified under ISO VG 150. The substitution of ester bond with tertiary amide bond contributed to the higher kinematic viscosity due to branched dibutylamine moiety that increased intermolecular chain entanglement as well as the higher polarity of the amide bond, which led to the observed increment of kinematic viscosity. Based on its kinematic viscosity, DBALaE can be used as a base oil for gear oil that requires higher viscosity for better prevention of friction and wear. For the same reason of intermolecular chain entanglement, the reported triglycerides-based estolide (DOPO) exhibited even higher kinematic viscosities at 40°C (417 cSt) due to its triglycerides molecular structure and the use of oleic acid as an end-capping fatty acid.

Viscosity index (VI) is another important feature of a lubricant, in which a high VI number suggests that the viscosity of the lubricant is less affected by changes in temperature and *vice versa*. In accordance with the commercial standard, a good lubricant will exhibit a VI value above 100. Both prepared 2EHLaE and DBALaE can be considered good lubricants in terms of VI as they displayed VI values of 190 and 169, respectively, which were significantly higher than the commercial sample HLP68. Both TMPTE and DOPO also showed good VI numbers above 100 as bio-lubricants are known to have good VI attributes (Cecilia *et al.*, 2020).

Another important aspect of a lubricant is the cold flow characteristic which can be determined by measuring the pour point of the lubricant. The pour point is described as the lowest temperature at which the lubricant ceases to flow, which signifies the lower limit of the lubricant operational temperature. The high pour point of palm oil-based lubricants is a major hindrance that limits their market acceptance in countries with cold climates and chemical modification of palm oil is required to achieve an acceptable pour point (Erhan *et al.*, 2006).

Referring to *Table 2*, the commercial lubricant HLP68 exhibited a pour point of -6°C, which represented the acceptable pour point in the lubricant market. Conversely, the TMPTE made from palm oil can only achieve a pour point of 9°C due to the molecular structure of TMPTE and the high content of saturated fatty acids in TMPTE that originated from palm oil. In comparison, both synthesised 2EHLaE and DBALaE exhibited a pour point of -12°C, which was significantly better than TMPTE and HLP68. The substantial improvement in pour point shown by 2EHLaE and DBALaE can be attributed to the branched structure of 2EHLaE and DBALaE that hindered molecules from packing albeit having a similarly high content of saturated fatty acids as compared to TMPTE. In contrast, the DOPO can only achieve a pour point of -5°C due to its triglycerides molecular structure even though it has estolide moieties, which significantly improved its pour point in comparison with starting material palm olein.

The oxidation stability of a lubricant at a high operating temperature is another important quality that can be measured using the pressure differential scanning calorimetry (PDSC) method. A lubricant with good oxidation stability will show a high oxidation onset temperature (OOT) and *vice versa*. Palm oil-based lubricants have lower oxidation stability due to inherent alkene groups that are susceptible to oxidation degradation. Therefore,

the palm-based TMPTE and DOPO that contained significant alkene groups exhibited OOT of 183°C and 156°C, respectively, which were inferior to both 2EHLaE and DBALaE that showed a higher OOT of 200°C due to the conversion of alkene groups to oxidation stable functional groups as seen in the synthesis of 2EHLaE and DBALaE. Furthermore, both 2EHLaE and DBALaE displayed similar oxidation stability as compared to commercial sample HLP68.

One of the main functions of lubricant is to minimise friction between two surfaces in close contact by the formation of a lubricating layer that prevents wear. Generally, a lubricant with excellent anti-wear quality will display a small wear scar diameter when evaluated in accordance with ASTM 4172 standard method. Referring to *Table 2*, both synthesised samples 2EHLaE and DBALaE exhibited slightly smaller wear scar diameters (0.58 mm and 0.56 mm, respectively) in comparison with commercial mineral oil (0.60 mm), which suggested that the anti-wear properties of 2EHLaE and DBALaE were comparable to the commercial product.

One of the main advantages of bio-lubricant is its inherent good biodegradability, which ensures the lubricant product is environment-friendly. On top of that, most bio-lubricants are made from renewable resources, which contribute to sustainable product development. Specifically, an earlier study on the biodegradability of estolide ester and amide (Hoong *et al.*, 2020), reported that 2-ethylhexyl ester of estolide and dibutyl amide of estolide were readily biodegradable. Hence, the prepared 2EHLaE and DBALaE of this study should have the same biodegradability performance as those estolide ester and amide reported in the literature since they have the same molecular structures albeit different fatty acid compositions, which ensure the environmental-friendly feature of the prepared 2EHLaE and DBALaE.

## CONCLUSION

Analyses conducted on palm-based UCO showed that it had higher free fatty acid, moisture and saturated fatty acids content as compared to fresh cooking oil (RBDPOo). Nonetheless, the UCO was found to have an adequate amount of unsaturated fatty acids that enable it to be used as feedstock to produce estolide ester and amide.

In the process of making estolide ester and amide, the UCO was converted to a mixture of fatty acids, which was then reacted with acetic acid and hydrogen peroxide to yield an estolide mixture with hydroxyl and carboxylic acid groups. Subsequently, the hydroxyl groups of the estolide mixture were end-capped with fatty acids while

its carboxylic acid groups were converted to either ester or amide functionalities, which eventually afforded 2EHLaE and DBALaE with a saturated branched structure.

Physicochemical properties evaluation revealed that the saturated branched structure of 2EHLaE and DBALaE contributed to better cold flow properties and enhanced oxidation stability in comparison with starting material UCO. Overall, this study demonstrated that the drawbacks of palm-based UCO lubricants such as inferior cold flow and oxidation stability properties can be improved through chemical modification performed on UCO that generated 2EHLaE and DBALaE, which displayed lubricant properties comparable with commercial lubricants. Additionally, the prepared 2EHLaE and DBALaE should exhibit good biodegradability, which ensures their suitability as an environment-friendly bio-lubricant.

## ACKNOWLEDGEMENT

The authors would like to thank the Director-General of MPOB for permission to publish this article. We would like to thank the following personnel for analyses conducted on samples: Selasiah Abdullah, Ahmad Lutfi Md Yusof, Sapia Hashim, Bahriah Bilal, Makmor Abd. Wahab, Norizan Ali, Mohd Zambri Yusof and Mohd Taib Samsudin.

## REFERENCES

- Ahmed, R B and Hossain, K (2020). Waste cooking oil as an asphalt rejuvenator: A state-of-the-art review. *Constr. Build. Mater.*, 230: 116985.
- American Oil Chemists' Society (AOCS), 2009. Acid value Te 1a-64; hydroxyl value Cd 13-60; iodine value Cd 1d-92; saponification value Cd 3-25; oxirane oxygen content Cd 9-57; Preparation of methyl esters of fatty acids Ce 2-66. *Official Methods and Recommended Practices of the American Oil Chemists' Society*. 6<sup>th</sup> edition. AOCS Press, Champaign, USA. 1200 pp.
- Beran, E (2010). Effect of chemical structure on the hydrolytic stability of lubricating base oils. *Tribol. Int.*, 43: 2372-2377.
- Cecilia, J A; Plata, D B; Saboya, R M A; Luna, F M T; Cavalcante, C L and Castellon, E R (2020). An overview of the biolubricant production process: Challenges and future perspectives. *Processes*, 8: 257.
- Cermak, S C; Bredsguard, J W; Roth, K L; Thompson, T; Feken, K A; Isbell, T A and Murray, R E (2015).

- Synthesis and physical properties of new cocoleic estolide branched esters. *Ind. Crops Prod.*, 74: 171-177.
- Cheah, K W; Yusup, S; Chuah, L F and Bokhari, A (2016). Physico-chemical studies of locally sourced non-edible oil: Prospective feedstock for renewable diesel production in Malaysia. *Procedia Eng.*, 148: 451-458.
- Derawi, D and Salimon, J (2013). Palm olein based biolubricant basestocks: Synthesis, characterization, tribological and rheological analysis. *Malaysian J. Anal. Sci.*, 17: 153-163.
- Erhan, S Z; Sharma, B K and Perez, J M (2006). Oxidation and low temperature stability of vegetable oil-based lubricants. *Ind. Crops Prod.*, 24: 292-299.
- Heikal, E K; Elmelawy, M S; Khalil, S A and Elbasuny, N M (2017). Manufacturing of environment friendly biolubricants from vegetable oils. *Egypt. J. Pet.*, 26: 53-59.
- Hoong, S S; Arniza, M Z; Mariam, N M D N S; Armylisas, A H N; Ishak, S A; Ismail, T N M T and Yeong, S K (2020). Synthesis of estolide ester and amide from acetylated polyhydroxy estolide for lubricant base oil. *Eur. J. Lipid Sci. Technol.*, 122: 2000098.
- Hoong, S S; Arniza, M Z; Mariam, N M D N S; Armylisas, A H N; Tang, S W; Ismail, T N M T and Yeong, S K (2021). Synthesis and physicochemical properties of new estolide esters as potential biolubricant base oil. *J. Oil Palm Res.*, 34: 152-166.
- Isbell, T (2011). Chemistry and physical properties of estolides. *Grasas Y Aceites*, 62: 8-20.
- Kalla, R M N; Choi, J S; Yoo, J W; Byeon, S J; Heo, M S and Kim, I (2014). Synthesis of 2-amino-3-cyano-4H-chromen-4-ylphosphonates and their anticancer properties. *Eur. J. Med. Chem.*, 76: 61-66.
- Kulkarni, M G and Dalai, A K (2006). Waste cooking oil – an economical source for biodiesel: A review. *Indian Chem. Eng.*, 45: 2901-2913.
- Lam, M K; Lee, K T and Mohamed, A R (2010). Homogeneous, heterogeneous and enzymatic catalysis for transesterification of high free fatty acid oil (waste cooking oil) to biodiesel: A review. *Biotechnol. Adv.*, 28: 500-518.
- Lee, S Y; Park, J W; Yoo, Y T and Im, S S (2002). Hydrolytic degradation behaviour and microstructural changes of poly(ester-co-amide)s. *Polym. Degrad. Stab.*, 78: 63-71.
- Li, W M and Wang, X B (2015). Bio-lubricants derived from waste cooking oil with improved oxidation stability and low-temperature properties. *J. Oleo Sci.*, 64: 367-374.
- Loh, S K; Choo, Y M; Cheng, S F and Ma, A G (2006). Recovery and conversion of palm olein-derived used frying oil to methyl esters for biodiesel. *J. Oil Palm Res.*, 18: 247-252.
- Milano, J; Shamsuddin, A H; Silitonga, A S; Sebayang, A H; Siregar, M A; Masjuki, H H; Pulungan, M A; Chia, S R and Zamri, M F M A (2022). Tribological study on the biodiesel produced from waste cooking oil, waste cooking oil blend with *Calophyllum inophyllum* and its diesel blends on lubricant oil. *Energy Rep.*, 8: 1578-1590.
- Nurazira, M N; Derawi, D and Salimon, J (2019). Esterification and evaluation of palm oil as biolubricant base stock. *Malays. J. Chem.*, 21: 28-35.
- Orjuela, A and Clark, J (2020). Green chemicals from used cooking oils: Trends, challenges, and opportunities. *Curr. Opin. Green Sustain. Chem.*, 26: 100369.
- Parveez, G K A; Tarmizi, A H A; Sundram, S; Loh, S K; Ong-Abdullah, M; Palam, K D P; Salleh, K M; Ishak, S M and Idris, Z (2021). Oil palm economic performance in Malaysia and R&D progress in 2020. *J. Oil Palm Res.*, 33: 181-214.
- Salimon, J; Salih, N and Yousif, E (2011). Chemically modified biolubricant basestocks from epoxidized oleic acid: Improved low temperature properties and oxidative stability. *J. Saudi Chem. Soc.*, 15: 195-201.
- Salimon, J; Salih, N and Yousif, E (2012). Biolubricant basestocks from chemically modified ricinoleic acid. *J. King Saud Univ. Sci.*, 24: 11-17.
- Sammaiah, A; Padmaja, K V and Prasad, R B N (2016). Synthesis and physical properties of novel estolides from dicarboxylic acids and methyl ricinoleate. *Eur. J. Lipid Sci. Technol.*, 118: 486-494.
- Schilt, A A (1979). *Perchloric Acid and Perchlorate*. The G. Frederick Smith Chemical Company, Columbus, Ohio, USA. p. 153.

Shahbandeh, M (2022). Vegetable oils: Global consumption 2013/14 to 2021/2022, by oil type. <https://www.statista.com/statistics/263937/vegetable-oils-global-consumption/>, accessed on 6 March 2022.

Wang, E P; Ma, X; Tang, S Z; Wang, Y; Wiley, W W and Reaney, M J T (2014). Synthesis and oxidative stability of trimethylolpropane

fatty acid triester as a biolubricant base oil from waste cooking oil. *Biomass Bioenergy*, 66: 371-378.

Zhang, W; Ji, H R; Song, Y L; Ma, S; Xiong, W; Chen, C J; Chen, B Q and Zhang, X (2020). Green preparation of branched biolubricant by chemically modifying waste cooking oil with lipase and ionic liquid. *J. Clean. Prod.*, 274: 122918.